

HYDRODYNAMIC MODELING OF PORT FOSTER, DECEPTION ISLAND (ANTARCTICA)

Juan Vidal* Manuel Berrocoso** Bismarck Jigena**

* *Centro Andaluz de Ciencia y Tecnologías Marina, Campus
Universitario de Puerto Real, Puerto Real (Cadiz) 11510 Spain
(e-mail: juan.vidal@uca.es).*

** *Laboratorio de Astronomía, Cartografía y Geodesia, Facultad de
Ciencias, Campus Universitario de Puerto Real, Puerto Real (Cadiz)
11510 Spain.*

Abstract:

A numerical, non-linear, barotropic, two-dimensional tidal model was implemented and used to simulate the M_2 , S_2 , O_1 and K_1 constituents in Port Foster (Deception Island, Antarctica). The model has been validated by comparing the simulation results against measured water levels data collected in several stations inside the domain. Once the model has been validated, the total volumen of Port Foster is exchanged with Bransfield Strait during the flood and the ebb tide have been estimated.

Keywords: Deception Island, model, Tides, Antarctica.

1. INTRODUCTION

Deception Island is part of the South Shetland Island chain with Smith, Snow and Livingston Islands to the north and west, and King George Island to the north and east. These islands form the northern boundary of the Bransfield Strait and the Antarctic Peninsula forms its southern boundary. Deception island is situated between latitudes 62.89 - 63.02 degrees South and longitudes 60.49 -60.75 degrees West. Deception Island is an active volcano that has a central flooded caldera, which is open onto Bransfield Strait through a shallow and narrow sill, at Neptune's Bellows, Smith Jr. et al (2003).

Bransfield Strait tides are a mixture of diurnal and semidiurnal frequencies. The M2 component is the most important with an amplitude around 0.40 m while O1, K1 and S2 tidal components, all with amplitudes around 0.28 m, are also significant, Lopez et al (1999). Amplitudes of the main tidal constituents are higher in the northwestern Weddell Sea than at the northwestern side of the peninsula, Dragani et al (2004). The local circulation in the Bransfield Strait is strongly influenced by tides. Both at the surface and at deeper layer, the flow patterns exhibit a strong diurnal and semidiurnal periodicity in agreement with the barotropic character of tides, Lopez et al (1994). The Bransfield Current is a northeastward geostrophic current. Based on geostrophic studies calculated to a reference level, various authors proved that the currents are oriented parallel to the front with speeds from 0.05 to 0.30 ms^{-1} , Niiler et al (1991) and Garcia et al (2002).

However, Port Foster water mass characteristics differ significantly from Bransfield Strait water mass characteristics, indicating that the sill at Neptunes Bellow limits cross-sill exchange below 30 m. The small tidal currents

in Port Foster, less than 0.1 ms^{-1} , also suggest that the larger Bransfield Strait tidal currents do not direct water into Deception Island, Lenn et al (2003). The maximum tidal currents are obtained at Neptune's Bellows, with 0.64 ms^{-1} during spring tides, Antarctic Pilot (1994).

Several hydrodynamical numeric models, including the Bransfield Strait have been recently implemented by several authors, Dragani et al (2004) and Padman et al (2002). However, these models are larger in scale.

The main objectives of this paper are to present a detailed study of the tidal characteristics in Por Foster. The tidal simulations are a first step towards the modeling of the whole island circulation.

The amplitudes and phases obtained through the analysis of the times series generated by the model allowed the attainment of co-tidal maps and ellipses of currents maps; these results were compared with the harmonic constants of several coastal stations, which positions are given in Fig 1. Based on the tidal maps, characteristics of the tidal propagation in the area are discussed.

2. MODEL APPROACH

The hydrodynamic model UCA2D here applied has been developed at University of Cadiz. A completed description of the model can be found in Alvarez (1999). It has already been applied successfully to several coastal environments. See, Alvarez et al. (1997), Alvarez et al (1999) and Vidal (2002).

2.1 Governing equations

The model resolves the equations in their formulations with water levels and transports:

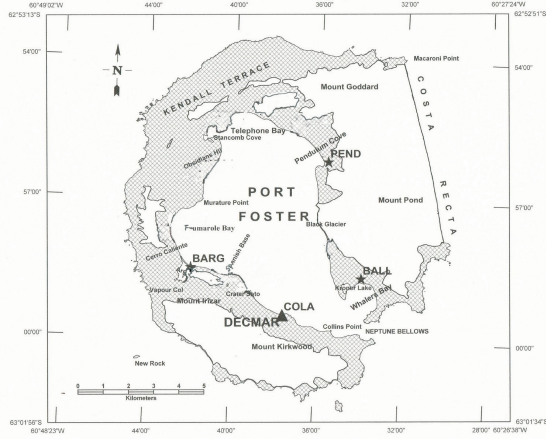


Fig. 1. Tidal Stations in Deception Island: (BALL) Balleneros Station, (COLA) Colatinas Sation and (PEND) Pendulo station

$$\frac{\partial U}{\partial t} - fV + gH \frac{\partial \zeta}{\partial x} + RU + X = 0 \quad (1)$$

$$\frac{\partial V}{\partial t} + fU + gH \frac{\partial \zeta}{\partial y} + RV + Y = 0 \quad (2)$$

$$\frac{\partial \zeta}{\partial t} + \frac{\partial U}{\partial x} + \frac{\partial V}{\partial y} = 0 \quad (3)$$

where f is the Coriolis parameter, ζ is the water level, g is the gravitational acceleration, $H = h + \zeta$ is the total water depth, and U and V are the vertically-integrated velocities. R is the friction coefficient which is expressed as:

$$R = C_b \frac{\sqrt{u^2 + v^2}}{H} \quad (4)$$

where C_b is the bottom drag coefficient. The terms X and Y of equations contain the nonlinear terms:

$$X = u \frac{\partial U}{\partial x} + v \frac{\partial U}{\partial y} - A_H \left(\frac{\partial^2 U}{\partial x^2} + \frac{\partial^2 U}{\partial y^2} \right) \quad (5)$$

$$Y = u \frac{\partial V}{\partial x} + v \frac{\partial V}{\partial y} - A_H \left(\frac{\partial^2 V}{\partial x^2} + \frac{\partial^2 V}{\partial y^2} \right) \quad (6)$$

where the last terms in equations represent the horizontal turbulent diffusion and A_H is the horizontal eddy viscosity.

At the open boundaries the water levels are prescribed in accordance with the Dirichlet condition, while at the closed boundaries the normal velocity is set to zero and the tangencial velocity is a free parameter.

3. APPLICATION TO PORT FOSTER

3.1 The model setup

The numerical computation has been carried out on a spatial domain that represents Port Foster through a finite element grid which consists of 7980 rectangular elements with a resolution of 100 m x 100 m (Figure 2). The bottom drag coefficient has been set to $cd = 3.0 \cdot 10^{-3}$. In barotropics models, the bottom drag coefficient is usually determined by fitting the modeled M2 tidal elevation and the observations as tide gauge stations, Crean et al (1988). All simulations presented in this work have been carried out using a maximum time step of 5 s.

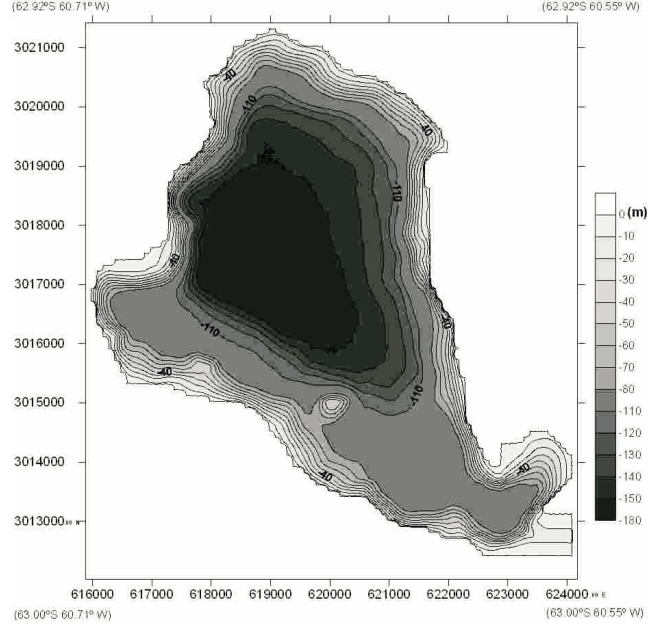


Fig. 2. Grid of Port Foster

The open boundary oscillations of the model consider components M2, S2, O1 and K1, that represent more than 90 % of the tidal energy in Port Foster, Lopez et al (1999). We use the amplitude and phase of the major tidal constituents from Antarctic Tide Gauge Database (<http://www.esr.org>) at the oceanic border.

For simulations of tidal velocities all variables, including sea levels and velocities were initially set to zero, and the model was forced at the open boundary by specifying the sea level as above.

3.2 Water level

The model has been validated comparing the amplitudes and phases of the major components generated by the model with those derived from harmonic analysis of the tide gauge data within the island Vidal et al (2010).

For each constituent of each simulation, the error in the amplitudes (e_A) and the error in the phases (e_F) were calculated using (7) and (8)

$$e_A = \sqrt{\frac{1}{N} \sum_i (A_{oi} - A_{mi})^2 / 2} \quad (7)$$

$$e_F = \frac{1}{N} \sum_i A_{mi}^2 (\theta_{oi} - \theta_{mi}) / (\sum_i A_{mi}^2) \quad (8)$$

where the error in the amplitudes was calculated from the difference between the observations (A_{oi}) and the results (A_{mi}) of the model, and the error in the phases was calculated from their difference ($\theta_{oi} - \theta_{mi}$), but weighted with the values of the observed amplitudes (A_{mi}).

4. RESULTS

Table 1 presents the comparison of the analysis of model results (M) with harmonic constants (O) of coastal stations (Balleneros, Pendulo and Colatinas). The tidal amplitudes are in meters and the phases angle are in degrees relative to local time.

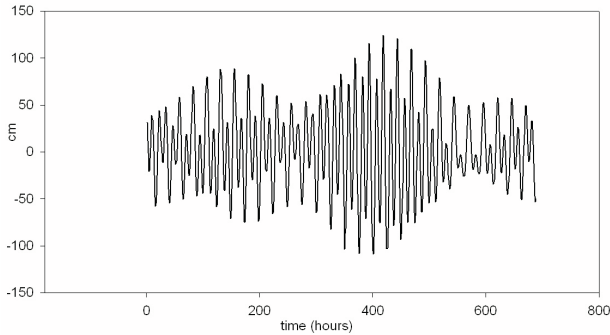


Fig. 3. Tidal elevation data obtained by the model

Model results show that the amplitudes of the components decrease as they spread into the caldera from the ocean, through Neptune's Bellows. The phase lags are also important in this area due to increased friction. Inside Port Foster, where depths are around 100 meters deep, the amplitudes and phase lags do not vary significantly.

The most important results obtained by modeling are that the amplitudes of the velocities are very low (less than 5cm/s) within Port Foster, excluding the area of Neptune's Bellows. The velocities near the narrow channel of Neptune's Bellows shows that the east-west direction is more important than the north-south, coinciding with the orientation of the narrow passage. For this area, through which it produces all the water exchange between the caldera and the open ocean, the results for simulations of tidal velocities show maximum speeds of 0.76m/s during spring tides. Table 2 shows the amplitudes of the velocities for the east-west components of the main harmonic constituents in a center point of the narrow and near Cola Station.

The volume of the basin is approximately 3500Hm^3 and the cross-section at Neptune's Bellows is about 6000m^2 . Figure 3 shows tidal elevation data obtained by the model at Neptune's Bellows. A mean tidal level variation is about 1.20 meter. A height of 1.20 m implies that about 1.10% of the total volumen of Port Foster is exchanged with Bransfield Strait during the flood and the ebb tide. The maximum range, defined as the largest difference (at spring) between a maximum and the next minimum, is around 2.20m. For the case of spring tides, this amount is approximately 2.8% of the total volume.

5. CONCLUSION

The tide in Port Foster was satisfactorily reproduced for all cases studied in this work. Currents obtained with the model are very small inside, with maximum values of 0.76m/s in the area of the Neptune's Bellows.

Port Foster in Deception Island has a rate of poor water exchange (1% volume exchange over each tidal cycle). The region where most of the tidal energy is dissipated is the Neptune's Bellows. Approximately 90% of the total energy dissipates in this area.

Table 1. Elevations: Harmonic analysis results

Station	Ball		Pend		Cola	
	O	M	O	M	O	M
M2						
A(m)	0.46	0.39	0.44	0.39	0.40	0.40
θ (degrees)	280	284	281	285	281	283
S2						
A(m)	0.28	0.26	0.29	0.26	0.26	0.26
θ (degrees)	Not Obs.	356	Not Obs	357	351	355
O1						
A(m)	0.29	0.27	0.29	0.27	0.27	0.27
θ (degrees)	48	55	55	55	53	54
K1						
A(m)	0.26	0.30	0.26	0.30	0.30	0.30
θ (degrees)	66	75	73	75	74	75
error						
e_A		0.03		0.03		0.00
e_F		2		1		1

Table 2. Velocities: Harmonic analysis results

Station	Neptuno's Bellows	Cola
M2		
A(m/s)	0.40	0.10
θ (degrees)	27	33
S2		
A(m/s)	0.25	0.07
θ (degrees)	90	98
O1		
A(m/s)	0.13	0.05
θ (degrees)	148	156
K1		
A(m/s)	0.15	0.06
θ (degrees)	166	179

ACKNOWLEDGEMENTS

This work was possible thanks to the project CGL2005-0789-C03-01/ANT INVESTIGACIONES GEODESICAS, GEOFISICAS Y DE TELEDETECCION EN LA ISLA DECEPCION Y SU ENTRONO (PENINSULA ANTARTICA, ISLAS SHETLAND DEL SUR), financed by Spanish Ministry of Science and Technology through the National Program of Antarctic Research of Natural Resources. We would also like to thank the Las Palmas Crew and the members of the Spanish Antarctic Station Gabriel de Castilla for their collaboration during the surveying campaigns.

REFERENCES

- O. Alvarez. Simulación numérica de la dinámica de marea en la Bahía de Cádiz: análisis de las constituyentes principales, interacción marea-brisa e influencia del sedimentación en suspensión. *Ph. D. Thesis*, Universidad de Cádiz, Cádiz, 1999.
- O. Alvarez, A. Izquierdo, B. Tejedor, R. Maanes, L. Tejedor and B.A. Kagan. The Influence of Sediment

- Load on Tidal Dynamics, a Case Study: Cadiz Bay. *Estuarine, Coastal and Shelf Science*, 48:439–450, 1999.
- O. Alvarez, B. Tejedor and L. Tejedor. Simulación hidrodinámica en el rea de la Bahía de Cádiz. Análisis de las constituyentes principales. *IV Jornadas Españolas de Puertos y Costas.*, pages 125–136. Servicio de Publicaciones de la Universidad Politécnica de Valencia, Valencia, 1997.
- J. Vidal. Caracterización dinámica de la marea y del sedimento en el canal de Sancti Petri. *Ph. D. Thesis*, Universidad de Cádiz, Cádiz, 2002.
- Y. D. Lenn, T. K. Chereskin and R. C. Glatts Seasonal to tidal variability in currents, stratification and acoustic backscatter in a Antarctic ecosystem at Deception Island. *Deep-Sea Research II*, 50:1665–1683, 2003
- O. Lopez, M. A. Garcia, D. Gomis, P. Rojas, J. Sospedra and A. Sanchez-Arcilla. Hydrographic and hydrodynamic characteristics of the eastern basin of the Bransfield Strait (Antarctica). *Deep-Sea Research I*, 46:1755–1778, 1999.
- W. C. Dragani, E. E. D'onofrio, M. E. Fiore and J. O. Speroni. Propagación y amplificación de la marea en el sector norte de la Península Antártica. *V Simposio Argentino y Latinoamericano Sobre Investigaciones Antárticas*, Buenos Aires, 2004.
- Antartic Pilot. Comprising the coasts of Antarctica and all Islands Southward of the Usual Route of Vessels, 4th Edition *Hydrographer of the Navy, Taunton, Somerset*, 1994.
- M. A. Garcia, C. G. Castro, A. F. Rios, M. D. Doval, G. Roson, D. Gomis and O. Lopez. Water masses and distribution of physico-chemical properties in the western Bransfield Strait and Gerlache Strait during austral summer 1995/96. *Deep-Sea Research II*, 49:585–602, 2002.
- K. L. Jr. Smith, R. J. Baldwin, R. S. Kaufmann and A. Sturz. Ecosystem studies at Deception Island, Antarctica: an overview. *Deep-Sea Research II*, 50:1595–1609, 2003.
- O. Lopez, M. A. Garcia and A. S. Sanchez-Arcilla. Tidal and residual currents in the Bransfield Strait, Antarctica. *Ann Geophysicae* 12:887–902, 1994.
- P. P. Niiler, A. Amos and J. H. Hu. Water masses and 200m relative geostrophic circulation in the western Bransfield Strait region. *Deep-Sea Research A*, 38:943–959, 1991.
- L. Padman, H. A. Fricker, R. coleman, S. Howard and L. Erofeeva A new Tide Model for the Anatarctic Ice and Seas. *Annals of Glaciology*, 3:1–14, 2002.
- J. Vidal, M. Berrocoso and A. Fernandez Study of the tide in Deception and Livingston Islands (Antarctica). *Antarctic Science*, in press, 2010.
- P.B. Crean, T. S. Murty and J. A. Stronach Mathematical Modelling of tides and Estuarine Circulation: the Coastal Seas of Southern British Columbia and Washington State. *Coastal Estuarine Stud*, 30:471pp. Edited by M. J. Bowman et al, Washinton, 1991.

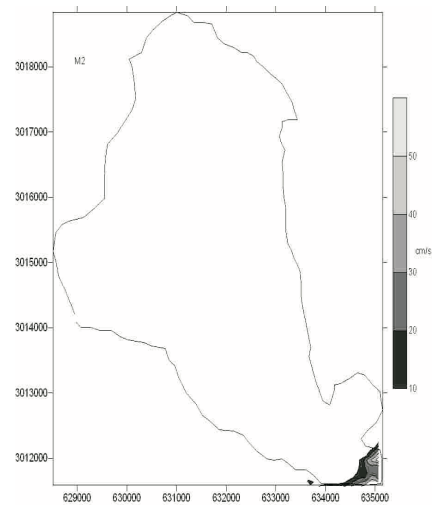


Fig. A.1. M2 velocities

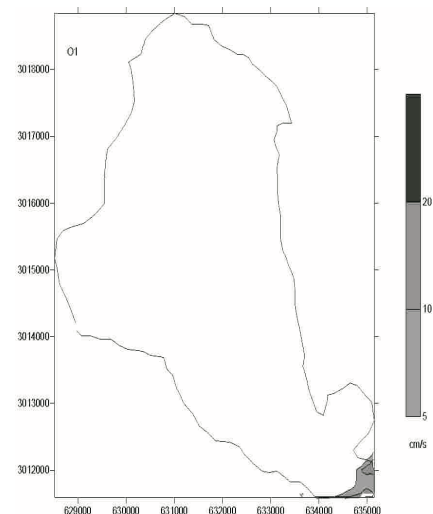


Fig. A.2. O1 velocities